European Journal of Forest Research
https://doi.org/10.1007/s10342-024-01699-5

RESEARCH

Enhancing precision in quantification and spatial distribution of logging residues in plantation stands

Alberto Udali[1] · Bruce Talbot[2] · Simon Ackerman[2] · Jacob Crous[3] · Stefano Grigolato[1]

Received: 29 November 2023 / Revised: 29 April 2024 / Accepted: 9 May 2024

Abstract

Forests, essential components of ecosystems, are managed for sustainable timber production in forest plantations to meet the growing demand for wood products. The intricate balance between sustainable forest management and logging residue management practices is crucial for ecological integrity and economic viability. Logging residues, byproducts of timber harvesting, significantly influence carbon and nutrient cycling, soil structure, and overall ecosystem health. Recent technological advancements, particularly the use of drones integrated with artificial intelligence, enable the processing of large datasets, providing meaningful insights into logging residues and forest dynamics. This study aims to evaluate the quantification and distribution of logging residues in forest plantations, utilizing machine learning classification models fed with drone-based images. The classification was performed using a Random Forest model fed with spectral and terrain variables, whereas the volume estimations were derived from field measurements and from the drone classification. Overall the classification achieved solid results (Overall Accuracy of 0.89), and the volume estimation resulting in solid comparison with field estimation (ratio 0.72–1.98), but poor correlation (R^2 of 0.26 and 0.36). We concluded that the proposed methodology is suitable for classifying and assessing residues distribution over recently harvested areas, but further improvement of the volume estimation methodology is necessary to ensure comprehensive and precise assessment of residue distribution over recently harvested areas.

Keywords Precision forestry · UAV · Artificial intelligence · Post-harvesting assessment · Management

Introduction

Forests are a vital component of our ecosystems, playing a crucial role in maintaining biodiversity, regulating climate, and providing resources essential for human sustenance (FAO 2020). As such, forest plantations, strategically managed for sustainable timber production, can contribute significantly to meeting the growing demand and sustainable use of wood products. Nowadays, in the management of forest plantations many practices are under review in order to meet more sustainable management goals, at local and global level (McEwan et al. 2020). Among these, the management of logging residues becomes paramount, influencing among other things both ecological integrity and economic viability.

Logging residues, i.e. the byproducts of timber harvesting, constitute branches, bark, foliage and other biomass materials left behind after the extraction of commercially utilizable timber (Harmon and Sexton 1996; Titus et al. 2021). Gaining a wider understanding of the role and the

Communicated by Miren del Río.

✉ Alberto Udali
alberto.udali@unipd.it

Bruce Talbot
bruce@sun.ac.za

Simon Ackerman
simona@merensky.co.za

Jacob Crous
jacob.crous@sappi.com

Stefano Grigolato
stefano.grigolato@unipd.it

[1] Department of Land, Environment, Agriculture and Forestry (TESAF), Università degli Studi di Padova, Legnaro, Italy

[2] Department of Forest and Wood Science, Stellenbosch University, Stellenbosch, South Africa

[3] Shaw Research Centre, Sappi Southern Africa Ltd, Howick, South Africa

Published online: 30 May 2024

dynamics of these residues is pivotal, as they influence Carbon, Nitrogen (Achat et al. 2015; James et al. 2021) and nutrient cycling (Janowiak and Webster 2010), soil physical structure (Trindade et al. 2021), biodiversity (Law and Kolb 2007; Fritts et al. 2017, Grodsky et al. 2019) and overall ecosystem health (Bose et al. 2023). The sophisticated array of options to consider involving the presence of residues and the possible dangers or risks for the forest ecosystem, e.g., forest fire and pests outbreaks among the others, demands thoughtful consideration in optimizing forest management practices.

The management of logging residues presents challenges that intersect the environmental and economic dimensions. Reaching a balance between these competing interests requires innovative solutions that address concerns related to soil degradation, carbon sequestration, and cost-effective management. In addressing these challenges, opportunities arise for advancements in technology and data-driven approaches.

In recent years, technological innovations have revolutionized forestry practices. Unmanned aerial vehicles (UAVs), commonly known as drones, have emerged as indispensable tools in the forestry sector. These aerial platforms offer a versatile means of data collection, enabling efficient monitoring of forested landscapes (Buchelt et al. 2024). Drones have found application in various facets of forest research, ranging from mapping, and monitoring to assessing tree health and biodiversity. Their ability to cover larger areas with speed and precision has redefined the possibilities for data collection. According to the analysis of Buchelt et al. (2024), drones are still not largely used in the realm of forest operations and harvesting, although they could contribute to our understanding of logging residue distribution (Udali et al. 2022), offering insights that were once challenging to obtain through conventional means. Moreover, the integration of Artificial Intelligence (AI), Machine Learning (ML), and Deep Learning (DL) into drone technology to process large datasets of stratified information marks a paradigm shift in data analysis (Ongsulee 2018). The synergy between drone capabilities and artificial intelligence opens new avenues for comprehensive and nuanced forest management.

This integration has already been experimented on in recent years within the realm of forest operations, achieving positive results. Windrim et al. (2019) used a Convolutional Neural Networks (CNNs) based technique to detect individual logs and stumps and to segment image surface between woody material and background. Their application did efficiently detect woody debris and stumps with an accuracy of 84% overall. Puliti et al. (2018) performed stump detection in photogrammetry collected from UAVs using an iterative region-growing approach, and their results achieved an accuracy of 68–80%. Đuka et al. (2023) compared butt-log volume estimation from field measurements and four photogrammetric approaches with the ultimate goal of optimizing timber transport and estimated log dimensions with high level of correlation ($R^2 \geq 0.88$) and fairly good volume relative bias (< 10%).

The aim of this study is to evaluate the quantification and distribution of logging residues in clear-felled plantation stands. In particular, the objectives are (i) to assess the distribution performed using a ML classification model feed with drone-based images, and (ii) to compare the volume estimated from the classified images with the volume obtained from in-field observation.

Materials and methods

Study sites

The study sites are all industrial forest plantations located in the KwaZulu-Natal province in South Africa (Fig. 1). The province possesses a varied yet verdant climate thanks to diverse, complex topography. The hinterland where the sites are located is characterized by a dry-winter humid subtropical climate, whereas summers are warm and occasionally hot, with frequent rainfall. Winters are dry with high diurnal temperature variation, with possible light air frosts (South African Weather Service).

The species planted on the sites are a hybrid clone of Eucalypt (*Eucalyptus grandis* W.Hill *x Eucalyptus nitens* (H. Deane & Maiden) Maiden), *E. dunnii* Maiden, *E. smithii* (R.T. Baker.) and Mexican weeping pine (*Pinus patula* Schiede ex Schltdl. & Cham.), hereafter identified as Eucalypt and Pine, respectively. The harvesting and extraction operations were performed in all sites in the year 2022, where the timber was either manually or mechanically felled and then transported by forwarder to depot. On the sites mechanically felled, the machine adopted was a Tigercat LH822D equipped with Log Max 7000XT head working with cut-to-length (CTL) technique, whereas the forwarder adopted was a Tigercat 1075C. Table 1 summarizes the main data related to the selected study sites.

Field sampling, target material and volume estimation

Field sampling of logging residues was performed by adopting a line intersect sampling (LIS) method, which estimates volumes of downed woody material (Brown 1974; Woodall and Monleon 2008) over completely clear-felled areas. The

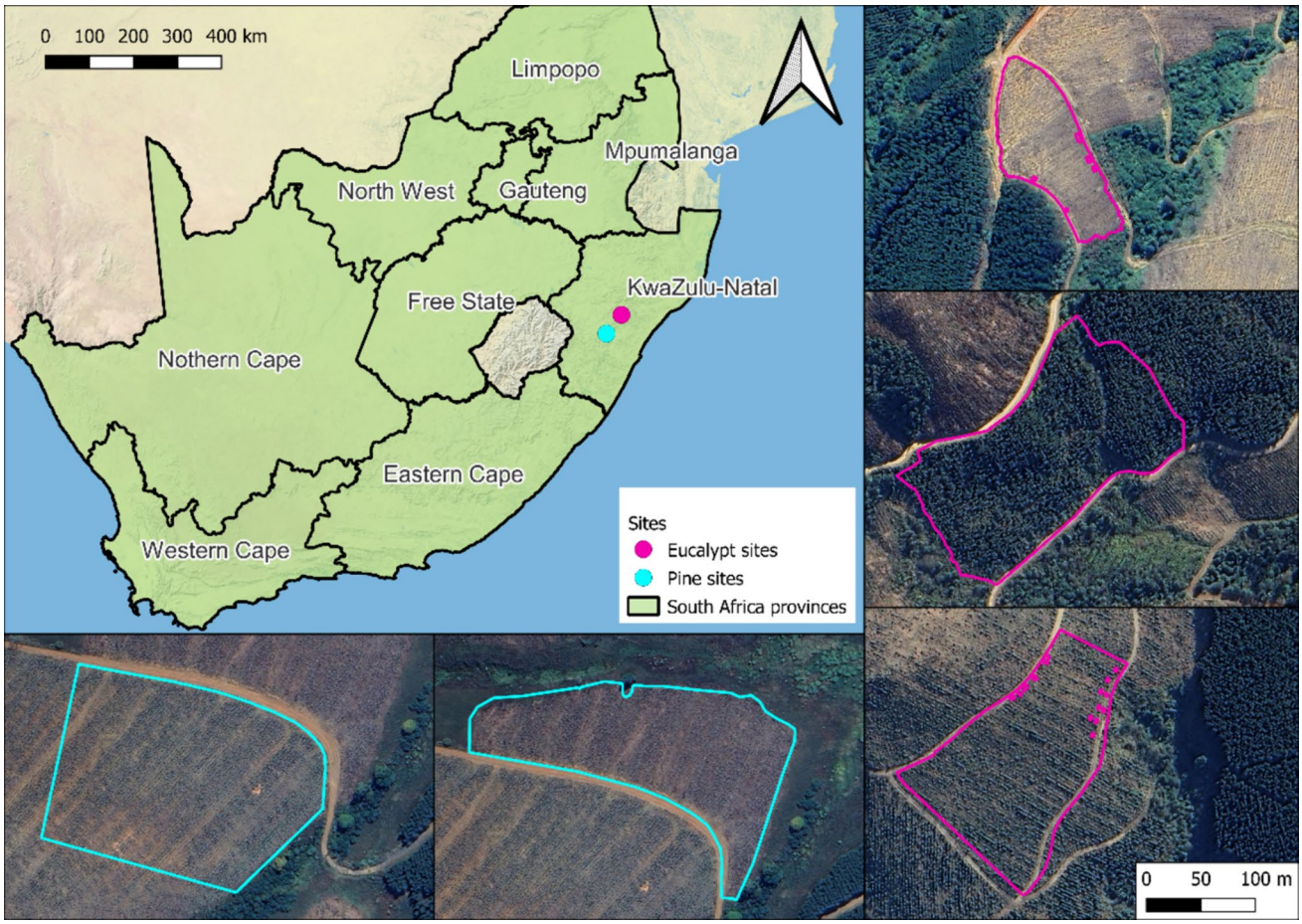

Fig. 1 Location of the study sites in South Africa. From the top right clockwise, Eucalypt sites E1, E2 and E3 followed by Pine sites P1 and P2. Background image from Google Satellite

Table 1 Summary of data related to the study sites selected

	E1	E2	E3	P1	P2
Average altitude (m a.s.l.)	1276	1090	1151	1107	1120
Aspect	NE	SE	SE	N	N
Surface (ha)	1.0	2.9	2.4	2.74	3.8
Number of plots	4	5	4	4	6
Genus planted	Eucalypt	Eucalypt	Eucalypt	Pine	Pine
Type of harvesting	Motor-manual felling Hand roll to roadside Forwarder to depot	Mechanical felling, CTL Forwarder to depot	Mechanical felling, CTL Forwarder to depot	Mechanical felling, CTL Forwarder to depot	Mechanical felling, CTL Forwarder to depot
Sites coordinates (WGS84)	29° 20′ 3.47″ S 30° 10′ 22.44″ E	28° 59′ 33.70″ S 30° 36′3 9.95″ E	29° 0′ 26.12″ S 30° 36′ 52.86″ E	29° 23′ 19.76″ S 30° 15′ 7.82″ E	29° 23′ 22.67″ S 30° 15′ 4.09″ E

main assumptions when using this sampling technique are the random orientation of the woody debris under the linear transect, lying horizontally, having a circular shape, and a normal distribution within diameter classes. To be able to

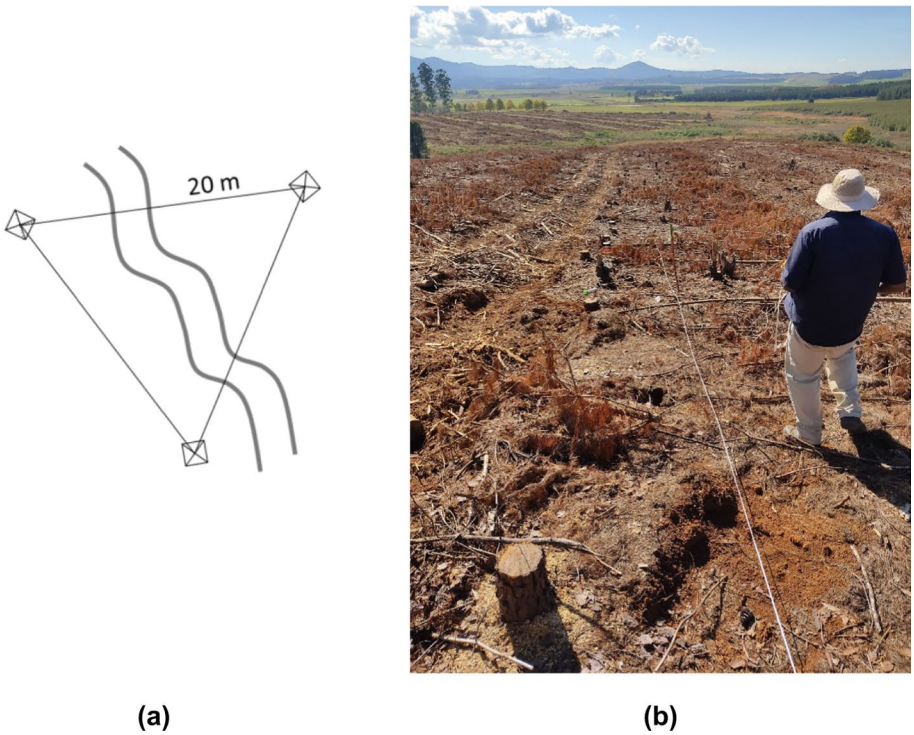

Fig. 2 Example of **a** transect layout and localization with respect to a hypothetical wheel rut, but could be applied generally; **b** transect over one of the Pine studies sites

cover each site, as "rule of thumb", a minimum ratio of 1.5 plot ha^{-1} was adopted to ensure enough coverage and representation of the area.

For this study, the sampling method (Fig. 2a) was initially adapted from Rizzolo (2016), registering the diameter of each piece of woody debris under a 20 m line and classifying them in time lag classes (Table 8). The plot, composed of three sampling lines disposed as a perfect triangle (Ross and du Toit 2004), has random orientation, with each triangle at least 25 m from other triangles and from the roadside. The time lag division of woody material refers to the time required for a fuel particle to change its moisture content accordingly to the equilibrium moisture content but can be easily adapted to other applications: material finer than 76 mm in diameter belongs to fine woody debris (FWD) and larger material to coarse woody debris (CWD). The length was also recorded for CWD larger than 203 mm.

The residue volume estimation (m^3 ha^{-1}) was performed for all categories of residues: for 1h, 10h, 100h and 1000h classes, the Brown's formula was used (Brown 1974; Woodall and Monleon 2008), described in Eq. (1). Whereas for bigger elements, the ones falling in the 1000 h+ class, the estimator was computed using the Woodall formula (Woodall and Monleon 2008), expressed by Eq. 3.

$$\hat{Y}_{ABCD} = \left(\frac{1.234 \cdot n \cdot \bar{d}^2 \cdot c \cdot a}{\sum L} \right) \cdot k_{decay} \cdot 10.000 \quad (1)$$

$$c = \sqrt{1 + \left(\frac{Slope_{\%}}{100} \right)^2} \quad (2)$$

$$\hat{Y}_E = \frac{\pi}{2L} \cdot \sum_{i=1}^{n} \left(y_i / l_i \right) \cdot k_{decay} \cdot 10.000 \quad (3)$$

where: 1.234 is a conversion constant derived empirically; n is the number of elements for each class; d is the average squared diameter for the class; c is the corrected slope (Eq. 2); a is the correction coefficient for the position of the elements, equal to 1.13 for FWD and equal to 1 for CWD; L is the length of the sampling line(s); *kdecay* is the decay coefficient as described by Woodall and Monleon (2008); 10,000 are the square meters in 1 ha; *yi* is the volume for the single CWD piece and *li* is the length of the piece.

UAV data acquisition and pre-processing

The whole methodology hereafter described is summarized in Fig. 3.

UAV based images were collected using a DJI Mavic Air 2S with a single flight at 65 m altitude with 80% forward and

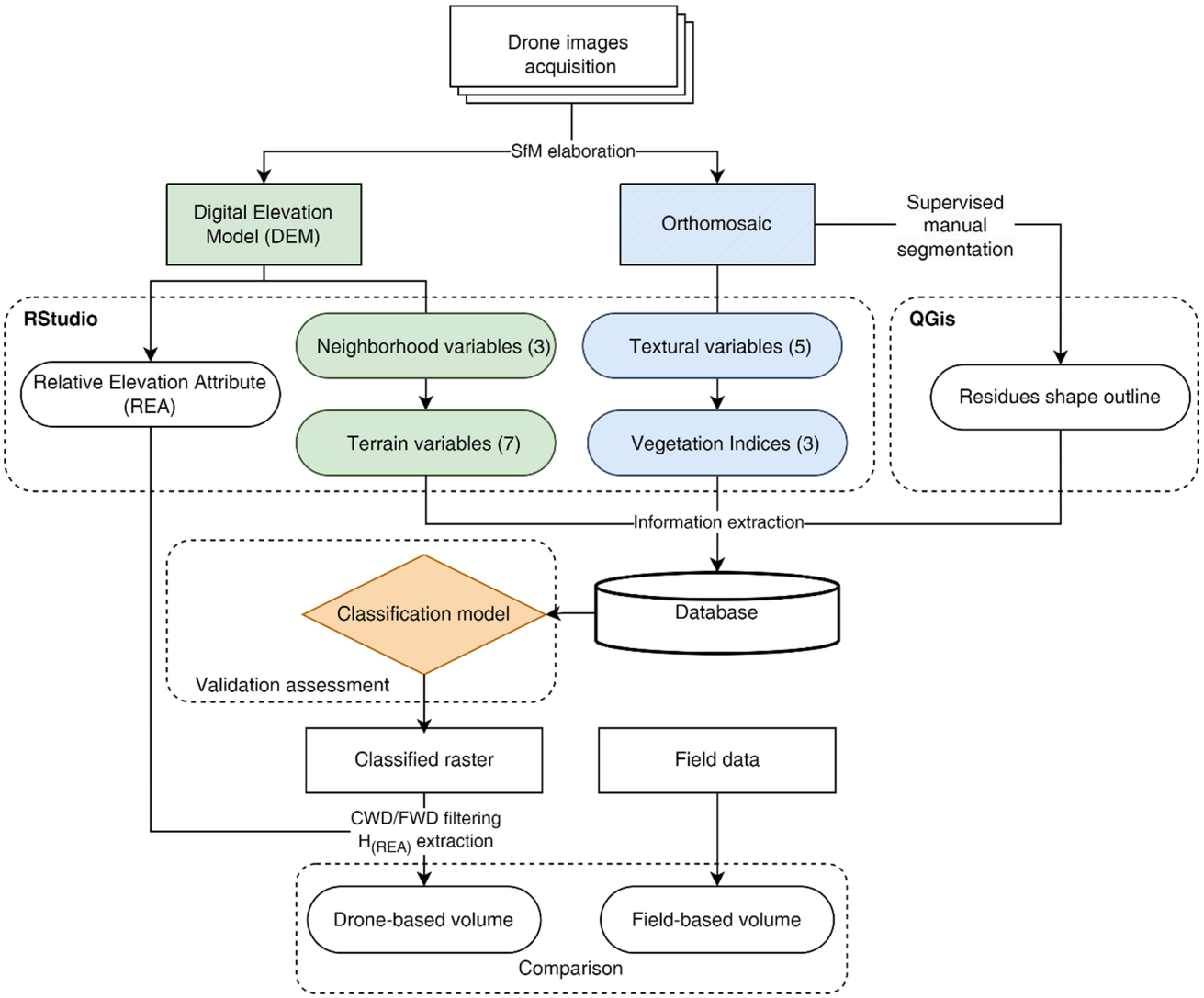

Fig. 3 Methodology workflow for this study, adapted from Udali et al. (2023)

Table 2 Number of sample grid areas laid out to visually interpret the objects from the orthomosaic for the classification algorithm

	E1	E2	E3	P1	P2	Total
Number of grids (10% of site area)	43	114	95	110	153	
Number of objects interpreted	736	986	675	449	605	3451
Number of pixels per class						
CWD	87,493	96,706	84,207	100,812	170,458	539,676
FWD	36,164	119,649	85,517	447,791	457,943	1,147,064
Ground	151,304	374 655	243 176	448 507	708 587	1,926,229
Stumps	6436	5500	3826	4867	5265	25,894

70% lateral overlap to cover the entire study site. The flights were performed in sky-clear, or under scattered cloud cover conditions. Ground Control Points (GCP) were positioned in the sites and the position of the points was recorded as well.

The images were pre-processed with a Structure-from-Motion (SfM) technique using Agisoft Metashape®: the sparse point cloud obtained from the images was georeferenced using the GCPs, optimized to reduce the reprojection errors and used to generate the dense cloud. From this last element, both the orthophoto and the Digital Elevation Model (DEM) were derived.

To build up the dataset for the classification model, similarly to Windrim et al. (2019), data related to logging residues was manually interpreted over the orthophoto in QGIS environment by placing a 5 × 5 m squared grid over the study area, and randomly selecting 10% of the grid cells to provide data for the model (Table 2). In the selected grid cells, objects were manually photo-interpreted, segmented and divided into 4 classes: Coarse Woody Debris (CWD), Fine Woody Debris (FWD), ground, and stumps. CWD was defined in this study as larger pieces of debris, clearly distinguishable from the background, as opposed to the smaller branches, foliage or bark (FWD). In this phase, all objects, when possible and clearly distinguishable, have been digitized in classes for the selected grid cells (Fig. 4). Moreover, merchantable timber left in the area in stacks has been filtered out and cropped from the images to avoid influencing either the classification or the volume estimation.

Table 3 Initial resolution (m) of orthomosaic and DEM obtained from Metashape for each study area

	E1	E2	E3	P1	P2
Initial orthomosaic resolution (m)	0.042	0.011	0.020	0.056	0.056
Initial DEM resolution (m)	0.084	0.023	0.041	0.056	0.056

Data elaboration

The following steps in the data elaboration were performed using R (R Core Team 2023) and RStudio environment (R version 4.2.3; RStudio 2023.06.0 + 421 "Mountain Hydrangea"). Prior to every elaboration, both the DEM and orthomosaic were resampled to a 3 cm resolution to match the minimum accountable dimension of residue of medium size (100 h), and to compare the volume estimations based on the same pixel area (Table 3).

In RStudio environment the DEM was used to calculate the roughness and the Terrain Ruggedness Index (TRI), which represent the largest inter-cell difference of a central pixel and its surrounding cell, and the mean difference between a central pixel and its surrounding cells, respectively (Wilson et al. 2007). Moreover, curvature variables were also considered to integrate the topographic information of the sites and to fully exploit the microtopography derived from the UAV-based DEM. In particular, the newly computed terrain variables consisted of slope, tangential

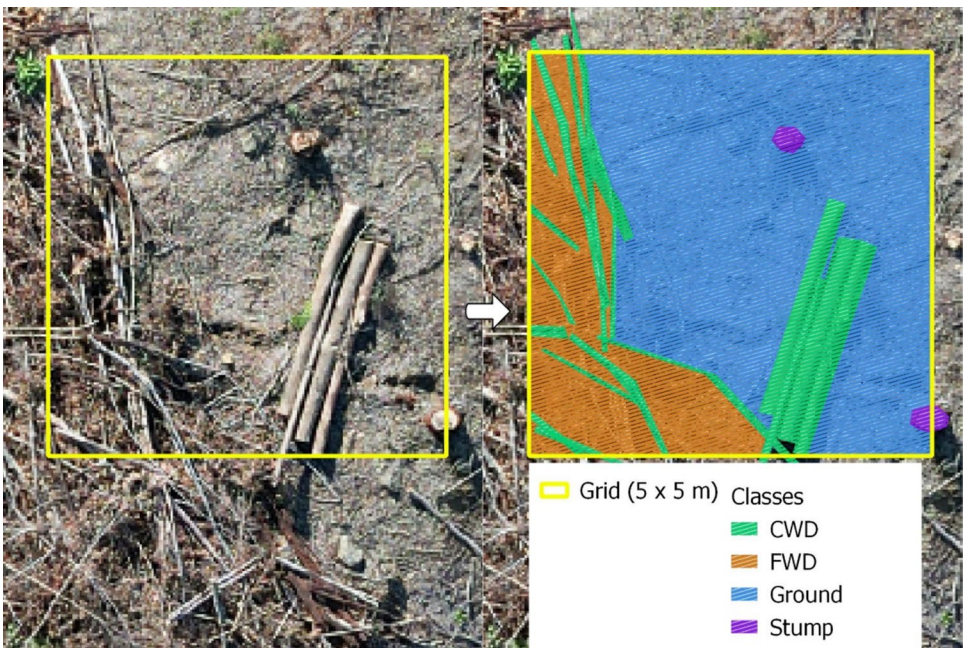

Fig. 4 Example of classes manual supervised segmentation over a 5 × 5 m grid cell

curvature, cross section curvature, minimum curvature, and profile curvature.

From the orthomosaic, the RGB values were extracted and used to compute textural variables for each one of the bands using the grey level co-occurrence matrix (*glcm*) function with window of size 3, producing 5 new accessory variables: mean, variance, homogeneity, contrast, and dissimilarity. Moreover, to account for the variability between the RGB singular layers, three vegetation indices were included: the normalized Green–Red difference Index (NGRDI), the Green–Blue Vegetation Index (GBVI), and the RGB Vegetation Index (RGBVI).

$$NGRDI = \frac{Green - Red}{Green + Red} \tag{4}$$

$$GBVI = \frac{Green - Blue}{Green + Blue} \tag{5}$$

$$RGBVI = \frac{2 \cdot Green - Red - Blue}{2 \cdot Green + Red + Blue} \tag{6}$$

Moreover, the DEM was also used to compute neighborhood variables to account the variability around the single pixels using the *focal* function from the R package *terra* (Hijmans 2023) and a moving window of size 5. This resulted in three new variables that accounted for the variability in the surface from the Digital Surface Model (DSM) considering the mean variation (mean_dsm), the variance (var_dsm) and standard deviation (std_dsm) for each singular pixel.

The textural variables, the vegetation indices, the neighborhood variables, and the terrain variables were all stacked together. The shapefile containing the interpreted residues was used to sample the variable values from the stack and were collected into a database.

Classification and validation

The database containing the variables was split following a 70/30 ratio for training and testing, respectively. First the training set was used to feed a Random Forest model to predict the class attribute, using the R package *randomForest* (Liaw and Wiener 2002). The prediction model used a total of 30 variables, using 5 of them (*mtry*) at each split and maintaining the default number of trees (*ntree* = 500).

The model obtained was then applied on the testing set and the results were expressed as a confusion matrix with accuracy indicators, as also suggested by Olofsson et al. (2014). In this case, the balanced accuracy for each class, the overall accuracy for the model and Kappa index (McHugh 2012) were derived directly from the model summary. Balanced accuracy refers to the average between the sensitivity (i.e. accuracy measured on the true-positive) and the specificity (i.e. accuracy measured on the true-negative) for each class. Model accuracy measures the number of correct predictions divided by the total number of predictions made. The Kappa index, which considers both the inter-rater and intra-rater reliability agreement among observations and observer, was used, in this case, to evaluate the effectiveness of the classification by comparing the agreement between the classification results and the expected values. The index was interpreted with the following guidelines (Landis and Koch 1977): value < 0 indicates no agreement, 0–0.20 as slight, 0.21–0.40 as fair, 0.41–0.60 as moderate, 0.61–0.80 as substantial, and 0.81–1 as almost perfect agreement.

The model was then used to classify the orthomosaic raster to visualize the residue distribution over the sites.

Volume calculation

To perform the volume computation, the CWD and FWD polygons were extracted from the classified raster, filtered by selecting the ones with at least 120 pixels connected for both FWD and CWD, and used to calculate the volume for each polygon following a "local difference-of-height approach".

The volume was then calculated using a Relative Elevation Attribute (REA) as described by Carturan et al. (2009): in this case the Digital Terrain Model (DTM) was interpolated using a low-pass filter to build a proxy for the terrain ($\overline{E}_{int}$) over the DSM (Straffelini et al. 2021); considering the

Table 4 Balanced class accuracy and model overall accuracy of the random forest models over the study sites

Sites	Balanced accuracy				Model OA	Model K-index
	CWD	FWD	Ground	Stumps		
E1	0.92	0.89	0.96	0.77	0.92	0.86
E2	0.83	0.84	0.88	0.65	0.86	0.78
E3	0.84	0.85	0.89	0.67	0.89	0.73
P1	0.80	0.92	0.94	0.60	0.90	0.90
P2	0.83	0.93	0.93	0.61	0.90	0.90
Average	0.84	0.89	0.92	0.66	0.89	0.83

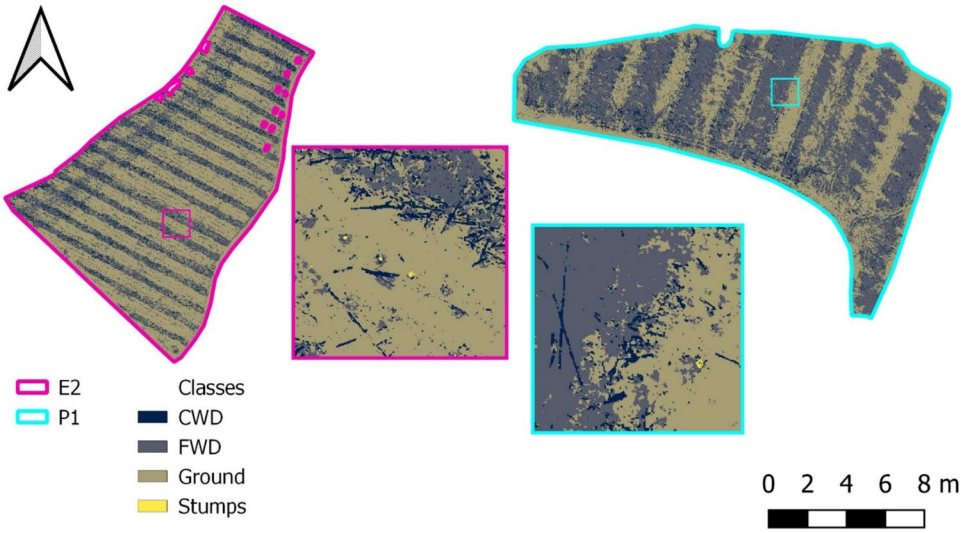

Fig. 5 Examples of classified sites output from the Random Forest models. The blank areas within the Eucalypt areas had merchantable timber not yet extracted and therefore masked out from the classification and volume estimation. Also, a close detail of the classification is depicted

Table 5 Average volume (m^3 ha^{-1}) for residues (FWD—fine woody debris, CWD—coarse woody debris) in the study sites divided for each class

Sites	FWD			CWD	
	1 h	10 h	100 h	1000 h	1000 h+
E1	2.41 (0.57)	18.03 (7.94)	14.19 (13.85)	19.47 (21.62)	34.94 (35.52)
E2	1.82 (0.57)	17.69 (4.96)	19.90 (11.26)	32.30 (19.35)	12.85 (21.44)
E3	1.53 (0.53)	12.22 (3.93)	11.82 (10.54)	35.53 (19.92)	26.10 (35.83)
P1	0.67 (0.25)	17.94 (4.54)	28.03 (13.83)	63.09 (30.69)	31.87 (32.66)
P2	0.81 (0.43)	23.26 (10.83)	24.54 (14.00)	71.17 (53.10)	28.10 (51.70)
Average eucalypt	1.92	15.98	15.30	29.10	24.63
Average pine	0.74	20.60	26.29	67.13	29.99

Standard deviation is also reported in brackets

Table 6 Volume (m^3 ha^{-1}) comparison between drone-based estimations and field-based estimators

Sites	Volume (m^3 ha^{-1})					
	FWD field-based	FWD drone-based	FWD volume ratio	CWD field-based	CWD drone-based	CWD volume ratio
E1	34.63	49.79	1.44	54.41	78.98	1.45
E2	39.41	46.64	1.18	45.15	36.07	0.80
E3	25.57	111.69	4.37	61.63	47.25	0.77
P1	46.64	72.15	1.55	94.96	24.54	0.26
P2	48.61	67.01	1.38	99.27	29.77	0.30
Average eucalypt	33.20	69.37	2.33	53.73	54.10	1.01
Average pine	47.63	69.58	1.46	97.12	27.15	0.28
R^2			*0.26*			*0.36*

R^2 is calculated as a linearcorrelation between Field-based volume and drone-based

Table 7 A comparison of results between the present study and previous studies available in literature

Studies	Accuracy			
	Overall accuracy	CWD	Stumps	Classification or segmentation method adopted
Present study	0.89	0.84	0.66	Random forest
Windrim et al. (2019)[a]	–	0.54	0.84	Faster RCNN
Puliti et al. (2018)[a]	–	–	0.68–0.80	Random forest
Shokirov et al. (2021)[b]	0.725	0.66	–	Random forest
	0.755	0.74	–	Random forest
	0.782	0.69	–	Random forest
Queiroz et al. (2019)[a,b]	–	0.76–0.87		Random forest

The main focus is put on CWD and Stumps, as common denominators for all the studies

[a]The class accuracy correspond to the overall accuracy since the model was developed to classify that specific object/target

[b]Studies that have used laser-borne data instead of SfM

resolution of the DEMs (0.03 cm) and due to the ruggedness of the terrain the filter was built with a kernel of 101×101 cells. In this case, compared to Straffellini et al. (2021) that were looking at differences in height due to local depressions in the terrain, the aim is to observe differences in height due to the presence of woody debris. Therefore, for each cell, the REA—in this case representing the height information of each cell—was obtained by subtracting the elevation value of the interpolated terrain from the DSM. This information then was extracted for each residue polygon and used to compute the volume (Eq. 5).

The drone-based volume was then compared to the field-based volume by producing a volume ratio.

$$REA = E_{DSM} - \overline{E}_{int} \tag{7}$$

$$Volume = A_{polygon} \cdot \overline{H}_{REA} \tag{8}$$

Results

Classification and validation

The balanced class and model overall accuracy (OA) over the study sites are presented in Table 4. Overall, the class presenting the higher accuracy is the one representing the Ground, identified with an average accuracy of 92% over the five sites. The second highest is the FWD class with 89%, followed by CWD and Stumps with 84% and 66% respectively. Considering the overall accuracy, the classification model achieved positive results for all the sites with values greater than 85% to a maximum of 92% for E1. In Fig. 5 the sites classified according to the models are presented, showing residue distribution over the harvesting areas.

Volume estimation and comparison

The estimated volume per hectare for each study area and divided by residue class is reported in Table 5. In general, Pine sites show a higher volume value for CWD for both classes compared to Eucalypt ones, especially for the 1000 h class. On the other hand, Eucalypt sites show higher volume values when it comes to the lowest diameter material (1 h class) to reduce the values for the following FWD classes. On average, on Pine sites a higher volume of material was left for almost all the residues classes considered, with the exception of the finer material, where more was present in Eucalypt sites, and the coarser material, where no large difference was present.

The volume obtained from drone-based approach is presented in Table 6, together with the site average volumes for CWD and FWD, and relative comparison. The comparison was computed by comparing the drone volume with the field volume. On average, more volume was detected and retrieved for FWD than CWD, with higher volume for Eucalypt sites for both residues categories.

Discussion

Classification and validation

The evaluation of accuracies showed that, overall, the proposed method achieved good results in classifying harvesting

residues in the study sites. The highest OA was achieved for E1, but it was also the site that was oversampled, in terms of number of plots per hectare (4 plot ha^{-1}), compared to the others (~ 1.5 plot ha^{-1}). If considering a division by tree species, the Pine sites showed, on average, better accuracy results when considering OA performances together with class accuracy FWD and Ground. This may be due to a more pronounced contrast in terms of light and color, used then from the classification model, between the different classes to distinguish them. Compared to other studies where the classification of harvesting residue was the main goal or just secondary aim, the presented model overall achieved good results (Table 7). Compared to previous research, the proposed approach produced a robust result in classifying CWD material with one of the highest accuracy values, whereas the performance in detecting stumps was more moderate, falling just outside of the range of values described by Puliti et al. (2018), maybe due to the difference in tree species as object of investigation. Compared to only the studies reporting the use of the same Random Forest model to classify CWD (Queiroz et al. 2019; Shokirov et al. 2021), the accuracy values presented in this study show higher results in both overall accuracy and class accuracy.

The results achieved in this study are in line and correspond with previous studies using UAV-based information combined with ML techniques, although with a very limited number of studies available. While using a more advanced and complex method compared to ML algorithms (Ongsulee 2018), Windrim et al. (2019) presented a Faster-RCNN method relying only on RGB-based variables, without accounting for terrain-based information. Also, Queiroz et al. (2019) have proposed a similar approach combining spectral and LiDAR information to feed a Random Forest model. A more comprehensive approach was presented by Puliti et al. (2018) in which their Random Forest model used a total of 31 variables including spectral (RGB and RGB-derived ones), dimensional and geometrical variables. On the other hand, Shokirov et al. (2021) have used only terrain related variables (e.g., slope, roughness, aspect, DSM, TPI and TRI) from different laser-based sources to feed their classification model. For this study, the classification model saw a combined use of spectral and terrain variables achieving the highest result in accuracy.

The model related Cohen's Kappa coefficient, overall ranging 0.73–0.90, interpreted as substantial to perfect agreement between the observed and classified values, provides a solid indication to the robustness of the designed classification model.

Considering the accuracy results, and the possible influence of the different variables, Table 9 reports the importance score for each variable related to each model application, therefore to each site; in particular, the score was computed for the 20 most used variables. Among the most used and with the highest score there are variables mainly related to terrain parameters (mean_dsm, min_curvature, and profile_curvature), followed by spectral variables such as NGRDI and GBVI. In this sense, it is possible to appreciate how the classifier preference sets on using terrain parameters to distinguish the elements in the area of interest before relying on spectral variables and their derivatives.

Volume estimation and comparison

The volume estimations obtained through the field survey are highly comparable with what is already presented in literature, for both tree genera considered. Regarding the Eucalypt sites, the volume estimations were not affected by the harvesting system. In their study, du Toit et al. (2000) estimated the potential residues amount of 40 dry t ha^{-1} over their study areas, which results in a volume of 78 m^3 ha^{-1} (if considering an average specific gravity for Eucalypt of 0.511 g cm^{-3}). These values are comparable with the values obtained from the study areas presented in this study. In another study, du Toit (2008) reported information about sites with different residues treatments from his own research and previous work (Bradstock 1981; Tandon et al. 1988; Hunter 2001; Campion et al. 2006). In his study he reported and compared, related to his specific aim, a range of residues (in this case branches and bark) values between 12.51 and 22.98 t ha^{-1}, in which the average of FWD from E1, E2 and E3 fit (17.69 t ha^{-1}, 20.14 t ha^{-1} and 13.07 t ha^{-1}, respectively).

On the other hand, the available information on Pine sites in the literature does not provide a clear comparison compared to Eucalypt. First of all because of the destination of the timber material: in this case, the pines were grown on a sawtimber regime, resulting in more heavy and bigger branches compared to the ones cultivated for pulp purposes. With regards to our data, they fit in between these two categories, as reported and defined by Ross and du Toit (2004), also considering the quantity of residues.

When comparing the drone-based estimations and the field-based estimations, the results show a clear division between the estimates obtained at species level. In general, FWD volume tends to be more overestimated (2.33 for Eucalypt and 1.46 for Pine) compared to CWD volume (1.01 for Eucalypt and 0.28 for Pine). In particular, on Eucalypt sites there is a higher degree of variation in volume estimation for both FWD and CWD between sites. For example, the drone-based estimation for E3 site produced an overestimation of 4 times compared to field volume, whereas CWD for E2 and E3 gets slightly underestimated (0.80 and 0.77, respectively).

These uncertainties may be attributed to two main reasons: (i) the choice of the specific pixel size as unit of investigation and (ii) the packing of residues. In the first case, the chosen resolution neglects the finer residues classes (1h and 10h), making it hard to assess their contribution to the volume estimation. In the second place, the packing of residues on layers poses an issue at both field and processing level: residues piled on top of each other are masking out material of the other classes, making it hard to get a correct volume estimation at the very end. Compared to previous research, Windrim et al. (2019) obtained a more positive outcome when it comes to CWD (R^2: 0.545–0.587), probably due to the different segmentation and elaboration methodology, more suitable to perform object detection and segmentation. Shokirov et al. (2021) results are more comparable to the ones obtained (R^2: 0.05–0.26) since they considered true positive-false positive together although they considered isolated CWD with only grass cover as background.

In general, there might be different reasons for the non-correspondence of the estimates.

i. *Classification errors*. In particular for the woody debris classes, considering the models average, there is between 8 and 20% of misclassification error present. This, as the first step of the presented methodology, could have dragged the uncertainties further down.
ii. *Resolution*. Compared to the drone-based estimates, the ones performed in the field were also designed to count the very fine material (Table A 1), which was not possible to perform with the remote sensed information, even after the resampling.
iii. *Terrain interpolation*. The proposed methodology from Straffellini et al. (2021) was developed and applied to areas with different land-use destinations, and characteristics. Therefore, in adapting the solution proposed by the authors the choice of the kernel size was dimensioned on the CWD size rather than a FWD pile, which would have resulted in a larger moving window, also increasing the computational time.
iv. *Packing of residues*. To adjust the differences between the two estimation techniques a residue packing ratio could have been applied to the measured volumes. However, to the extent of our knowledge, there are no specific packing ratio available in the literature for Eucalypt and Pine, yet. A valid example is provided by Hardy (1996) were the ratio were calibrated on different species but with similar characteristics to the ones presented in this study in terms of residues dimensions. However, applying the ratio to the data before mentioned would generate more errors since residues piles were not considered as a single unit in the field sampling. Still, the lack of a species specific packing ratio is an issue to be considered.

Conclusion

The main aim of this study was developed in two steps: (i) to assess the distribution of logging residues using a ML classification model fed with drone-based images, and (ii) to compare the volume estimated from the classified images with the volume obtained from in-field observation. The results indicate that the proposed methodology is suitable to evaluate the distribution of residues in the post-logging scenario with high overall accuracy (0.89), also when considering two different species with different characteristics. When it comes to volume estimation, this study proposed a novel approach relying entirely on UAV-borne images but also considering terrain-related variables. Overall it produced encouraging results with positive correlation, but could be improved by addressing the points mentioned beforehand (classification errors, resolution, terrain interpolation and packing of residues), especially the terrain interpolation from drone imagery and the development of a local packing ratio to correct the estimations. Moreover, results like this could help in making a better assessment of carbon stocks in harvesting sites implementing a carbon budget also considering the residues elements as temporary carbon reservoir. In the future, high resolution lidar DTMs will be more easily accessible and provide huge help developing the baseline for volume estimations.

Appendix

See Tables 8 and 9

Table 8. Time lag class distribution, with diameter (D) thresholds, and category for forest residues (FWD—fine woody debris, CWD—coarse woody debris) Brown (1974); Rizzolo (2016)

Class	D min (mm)	D max (mm)	Category
1 h	0	6	FWD
10 h	6	25	
100 h	25	76	
1000 h	76	203	CWD
1000 h+	> 203		

Table 9 Importance values of the 20 most used variables in the classification model

	E1	E2	E3	P1	P2
Blue	52.71	106.28	71.83		
Blue_contrast	61.91		92.43	34.46	35.17
Blue_dissimilarity					28.42
Blue_homogeneity		65.45	137.87	27.01	
Blue_mean	57.58	72.77	79.64	26.27	37.55
Blue_variance	59.75	127.75	86.75	31.25	
cross_sec_curvature	106.32	99.48	93.14	93.30	67.30
GBVI	132.31	115.18	106.63	31.41	39.45
Green		78.53			
Green_constrast			67.57	39.54	30.21
Green_dissimilarity					
Green_homogeneity			135.74		
Green_mean					28.23
Green_variance	53.25	94.24			
mean_dsm	236.28	164.40	179.76	173.53	130.36
min_curvature	108.48	228.27	158.46	56.57	83.10
NGRDI	172.38	120.42	100.95	89.78	89.01
profile_curvature	113.90	215.71	206.75	150.45	99.73
Red	65.16	78.01	73.96	35.16	47.52
Red_contrast			91.72	26.72	
Red_dissimilarity			73.96		
Red_homogeneity			157.75		
Red_mean	62.45	67.02			34.16
Red_variance	65.16	75.92			
RGBVI	81.41	132.98	84.62	70.47	68.86
roughness	71.66	67.02		45.60	52.12
slope	77.08			33.71	41.69
std_dsm	67.33	67.54	68.28	36.71	41.03
tang_curvature	109.57	100.52	81.78	64.87	50.92
TRI				46.40	45.71
var_dsm	67.33	67.02		42.00	38.67

The color scale (red-white-blue) highlights the percentile distribution among all the values: red = 10th percentile, white = 50th percentile; blue = 90th percentile. If the variable slot is empty, the variable was not included in the list but was still used in the model. The higher the score, the higher the importance.

Acknowledgements The study was supported by the European Union's HORIZON 2020 research and innovation programme under the Marie Skłodowska Curie grant agreement N° 778322 and by the Agritech National Research Center and received funding from the European Union Next-Generation EU (PIANO NAZIONALE DI RIPRESA E RESILIENZA (PNRR) – MISSIONE 4 COMPONENTE 2, INVESTIMENTO1.4—D.D. 103217/06/2022, CN00000022) within the Task 4.1.4 (Spoke4). The authors thank Dr. Steven Dovey and Thokozani Sithole for assisting with field data collection.

Author contributions Conceptualization, A.U., S.G. and B.T.; methodology, A.U. and B.T.; investigation, data curation and data collection, A.U., S.A., and J.C.; software and validation, A.U.; formal analysis, B.T.; writing—original draft preparation, A.U.; writing—review and editing, A.U., S.A., J.C., S.G. and B.T.; visualization, A.U., S.G. and B.T.; supervision, S.G. All authors have read and agreed to the published version of the manuscript.

Funding Open access funding provided by Università degli Studi di Padova within the CRUI-CARE Agreement.

Data availability The data and code presented in this study are available on request from the corresponding author.

Declarations

Conflict of interest The authors declare no conflict of interest.

References

Achat DL, Deleuze C, Landmann G et al (2015) Quantifying consequences of removing harvesting residues on forest soils and tree growth—a meta-analysis. For Ecol Manag 348:124–141

Bose T, Vivas M, Slippers B et al (2023) Retention of post-harvest residues enhances soil fungal biodiversity in Eucalyptus plantations. For Ecol Manag 532:120806. https://doi.org/10.1016/J.FORECO.2023.120806

Bradstock R (1981) Biomass in an age series of *Eucalyptus grandis* plantations. Aust for Res 11(2):111–127. https://pascal-francis.inist.fr/vibad/index.php?action=getRecordDetail&idt=PASCALAGROLINEINRA82X0254598

Brown JK (1974) Handbook for inventorying downed woody material

Buchelt A, Adrowitzer A, Kieseberg P et al (2024) Exploring artificial intelligence for applications of drones in forest ecology and management. For Ecol Manag 551:121530. https://doi.org/10.1016/J.FORECO.2023.121530

Campion JM, Nkosana M, Scholes MC (2006) Biomass and N and P pools in above- and below-ground components of an irrigated and fertilised *Eucalyptus grandis* stand in South Africa. Aust for 69:48–57. https://doi.org/10.1080/00049158.2006.10674985

Carturan L, Cazorzi F, Fontana GD (2009) Enhanced estimation of glacier mass balance in unsampled areas by means of topographic data. Ann Glaciol 50:37–46. https://doi.org/10.3189/172756409787769519

Creech MN, Katherine Kirkman L, Morris LA (2012) Alteration and recovery of slash pile burn sites in the restoration of a fire-maintained ecosystem. Restor Ecol 20:505–516. https://doi.org/10.1111/j.1526-100X.2011.00780.x

de Trindade AS, Ferraz JBS, DeArmond D (2021) Removal of woody debris from logging gaps influences soil physical and chemical properties in the short term: a case study in Central Amazonia. For Sci 67:711–720. https://doi.org/10.1093/forsci/fxab045

du Toit B (2008) Effects of site management on growth, biomass partitioning and light use efficiency in a young stand of *Eucalyptus grandis* in South Africa. For Ecol Manag 255:2324–2336. https://doi.org/10.1016/J.FORECO.2007.12.037

Đuka A, Papa I, Lovrinčević M et al (2023) Terrestrial vs. UAV-based remote measurements in log volume estimation. Remote Sens 15:5143. https://doi.org/10.3390/RS15215143

FAO (2020) Global forest resources assessment 2020: Main report. Rome

Fritts SR, Moorman CE, Grodsky SM et al (2017) Rodent response to harvesting woody biomass for bioenergy production. J Wildl Manag 81:1170–1178. https://doi.org/10.1002/jwmg.21301

Grodsky SM, Hernandez RR, Campbell JW et al (2019) Ground beetle (Coleoptera: Carabidae) response to harvest residue retention: implications for sustainable forest bioenergy production. Forests 11:48. https://doi.org/10.3390/F11010048

Hardy CC (1996) Guidelines for estimating volume, biomass, and smoke production for piled slash. In: USDA Forest Service—General Technical Report PNW

Harmon ME, Sexton J (1996) Guidelines for measurements of woody detritus in forest ecosystems

Hijmans RJ (2023) terra: spatial data analysis

Hunter I (2001) Above ground biomass and nutrient uptake of three tree species (*Eucalyptus camaldulensis*, *Eucalyptus grandis* and *Dalbergia sissoo*) as affected by irrigation and fertiliser, at 3 years of age, in southern India. For Ecol Manag 144:189–200. https://doi.org/10.1016/S0378-1127(00)00373-X

James J, Page-Dumroese D, Busse M et al (2021) Effects of forest harvesting and biomass removal on soil carbon and nitrogen: two complementary meta-analyses. For Ecol Manag. https://doi.org/10.1016/j.foreco.2021.118935

Janowiak MK, Webster CR (2010) Promoting ecological sustainability in woody biomass harvesting. J for 108:16–23. https://doi.org/10.1093/jof/108.1.16

Landis JR, Koch GG (1977) The measurement of observer agreement for categorical data. Biometrics 33:159. https://doi.org/10.2307/2529310

Law DJ, Kolb PF (2007) The effects of forest residual debris disposal on perennial grass emergence, growth, and survival in a ponderosa pine ecotone. Rangel Ecol Manag 60:632–643. https://doi.org/10.2111/06-034R4.1

Liaw A, Wiener M (2002) Classification and regression by randomForest. R News 2:18–22. https://journal.r-project.org/articles/RN-2002-022/RN-2002-022.pdf

McEwan A, Marchi E, Spinelli R, Brink M (2020) Past, present and future of industrial plantation forestry and implication on future timber harvesting technology. J for Res (harbin) 31:339–351. https://doi.org/10.1007/s11676-019-01019-3

McHugh ML (2012) Interrater reliability: the kappa statistic. Biochem Med (zagreb) 22:276–282. https://doi.org/10.11613/bm.2012.031

Olofsson P, Foody GM, Herold M et al (2014) Good practices for estimating area and assessing accuracy of land change. Remote Sens Environ 148:42–57. https://doi.org/10.1016/j.rse.2014.02.015

Ongsulee P (2018) Artificial intelligence, machine learning and deep learning. In: International Conference on ICT and Knowledge Engineering, pp 1–6. https://doi.org/10.1109/ICTKE.2017.8259629

Puliti S, Talbot B, Astrup R (2018) Tree-stump detection, segmentation, classification, and measurement using unmanned aerial vehicle (UAV) imagery. Forests 9:102. https://doi.org/10.3390/F9030102

Queiroz GL, McDermid GJ, Castilla G et al (2019) Mapping coarse woody debris with random forest classification of centimetric aerial imagery. Forests. https://doi.org/10.3390/F10060471

R Core Team (2023) R: a language and environment for statistical computing

Rizzolo R (2016) Fuel models development to support spatially-explicit forest fire modelling in Eastern Italian Alps. Università degli Studi di Padova

Ross TI, du Toit B (2004) Fuel load characterisation and quantification for the development of fuel models for *Pinus patula* in South Africa. Institute for Commercial Forestry Research (ICFR), Bullettin 1–24

Shokirov S, Schaefer M, Levick SR et al (2021) Multi-platform LiDAR approach for detecting coarse woody debris in a landscape with varied ground cover. Int J Remote Sens 42:9316–9342. https://doi.org/10.1080/01431161.2021.1995072

Straffelini E, Cucchiaro S, Tarolli P (2021) Mapping potential surface ponding in agriculture using UAV-SfM. Earth Surf Process Landf 46:1926–1940. https://doi.org/10.1002/ESP.5135

Tandon V, Pande M, Singh R (1988) Biomass estimation and distribution of nutrients in five different aged *Eucalyptus grandis* plantation ecosystems in Kerala state

Titus BD, Brown K, Helmisaari HS et al (2021) Sustainable forest biomass: a review of current residue harvesting guidelines. Energy Sustain Soc 11:1–32

du Toit B, Esprey LJ, Job RA et al (2000) Effects of site management in *Eucalyptus grandis* plantations in South Africa, Scottsville, South Africa

Udali A, Cucchiaro S, Lingua E, Grigolato S (2023) Digging up into windstorms aftermath: understanding the effect of harvesting systems on salvage logging wood residues spatial distribution. EGU Gen Assem 2023:1

Udali A, Talbot B, Puliti S et al (2022) Assessing the potential for forest residue classification and distribution over clear felled areas using UAVs and Machine Learning: a preliminary case study in South Africa. In: 2022 IEEE Workshop on Metrology for Agriculture and Forestry (MetroAgriFor). IEEE, Perugia, 3–5 November 2022, pp 160–163

Wilson MFJ, O'connell B, Brown C et al (2007) Multiscale terrain analysis of multibeam bathymetry data for habitat mapping on the continental slope. Mar Geodesy 30:3–35. https://doi.org/10.1080/01490410701295962

Windrim L, Bryson M, McLean M et al (2019) Automated mapping of woody debris over harvested forest plantations using UAVs, high-resolution imagery, and machine learning. Remote Sens (basel) 11:733. https://doi.org/10.3390/RS11060733

Woodall CW, Monleon VJ (2008) Sampling protocol, estimation, and analysis procedures for the down woody materials indicator of the FIA Program. Gen Tech Rep NRS-22 68